ACS OMEGA

http://pubs.acs.org/journal/acsodf

Article

Scaffold Hopping to Imidazo[1,2-*a*]pyrazin-8-one Positive Allosteric Modulators of Metabotropic Glutamate 2 Receptor

Ana I. de Lucas,* Juan A. Vega, Aránzazu García Molina, María Lourdes Linares, Gary Tresadern, Hilde Lavreysen, Daniel Oehlrich, Andrés A. Trabanco, and José M. Cid*

Cite This: *ACS Omega* 2021, 6, 22997−23006

Read Online

ACCESS | Metrics & More | Article Recommendations | Supporting Information

ABSTRACT: Glutamate hyperfunction is implicated in multiple neurological and psychiatric diseases. Activation of the mGlu2 receptor results in reduced glutamate release and decreased excitability representing a promising novel therapeutic agent for the treatment of disorders such as epilepsy, schizophrenia, mood, anxiety, and other neuropsychiatric disorders. We have previously reported substantial efforts leading to potent and selective mGlu2 PAMs from different chemical series. Herein, the discovery and optimization of a novel series of imidazopyrazinone mGlu2 PAMs are reported. This new scaffold originated from computational searching of fragment databases and comparison with our previously explored scaffolds. Optimization guided by our robust understanding of SAR from former series led to potent, selective, and brain-penetrant compounds.

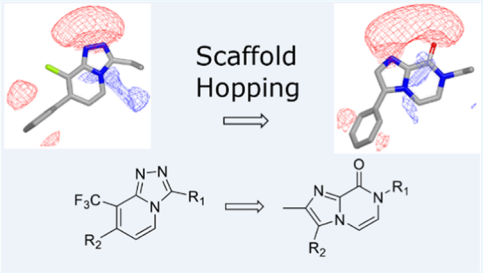

INTRODUCTION

Glutamate is a critical neurotransmitter influencing a broad range of physiological processes in the central nervous system (CNS) of vertebrates by binding to two families of receptors, the ligand-gated ion channels termed ionotropic glutamate (iGlu) receptors and G-protein-coupled receptors termed metabotropic glutamate (mGlu) receptors.[1,2] Of the eight mGlu receptor subtypes, the mGlu2 receptor subtype has proven to be of particular importance in neuropharmacology.[3−5] The mGlu2 receptor is expressed on presynaptic glutamatergic nerve terminals where it functions as an autoreceptor for glutamate.[6] Thus, its activation can normalize excessive glutamatergic neurotransmission leading to decreased excitability,[7] which may be of benefit in disorders such as epilepsy[8,9] and schizophrenia.[10,11] While efforts to develop highly selective mGlu2 orthosteric agonists failed due to the highly conserved glutamate binding site, targeting less conserved allosteric binding sites on the mGlu2 receptor led to unprecedented levels of the mGlu2 subtype selectivity with positive allosteric modulators (PAMs). A PAM also offers the benefit of increasing the affinity and/or efficacy of the endogenous neurotransmitter glutamate in a more physiologically tailored and saturable manner.

Within our laboratories, a long-lasting research effort in the $mGlu_2$ PAM field in collaboration with Addex Therapeutics resulted in the identification of our clinical lead JNJ 40411813 (**1**, Figure 1) from a series of pyridones.[12,13] Subsequent backup programs guided by scaffold hopping approaches led to the development of potent and selective imidazopyridine[14,15] and triazolopyridine mGlu2 PAMs.[16,17] More recently, we again showed how computationally guided scaffold hopping led to the discovery of a spirooxindole series of mGlu2 PAMs.[18]

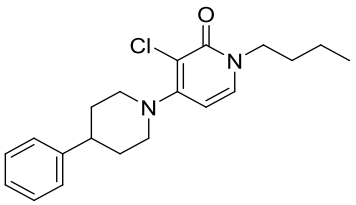

1, JNJ 40411813

mGlu2 PAM EC_{50} = 147 nM

mGlu2 PAM E_{MAX} = 273 %

Figure 1. Structure of the clinical mGlu2 PAM led to JNJ 40411813 (**1**).

To take full advantage of our large data sets and deep SAR understanding, a scaffold hopping exercise was conducted to further identify new chemotypes. Computational approaches using 3D shape and electrostatic similarity helped identify a new scaffold from triazolopyridine **2a** (Figure 2). The resulting new prototype **3a** (Figure 2) displayed encouraging mGlu2 PAM activity (EC_{50} = 490 nM). Likewise, the new hit **3a** exhibited reduced lipophilicity and more balanced in vitro clearance when compared with its corresponding matched triazolopyridine pair **2a**. Given the preliminary results, we examined whether the SAR could be transferable across series. Herein we report the exploration of the new imidazopyr-

Received: July 16, 2021
Accepted: August 10, 2021
Published: August 25, 2021

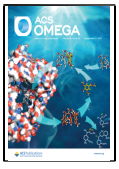

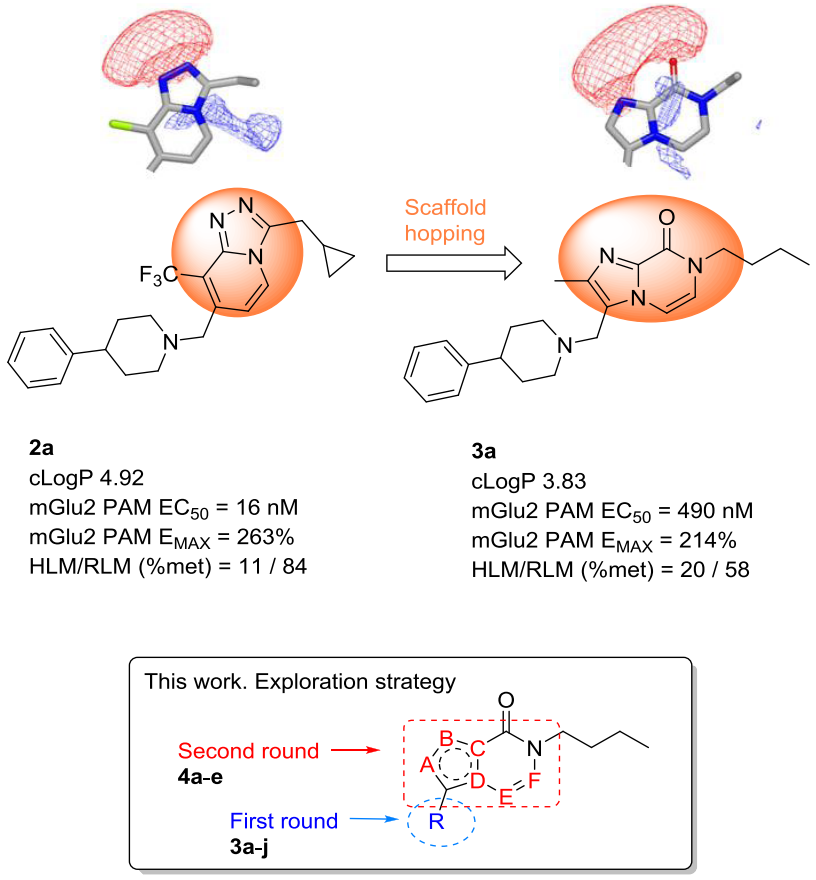

Figure 2. Scaffold hopping from triazolopyridine to the imidazopyrazinone core and exploration strategy.

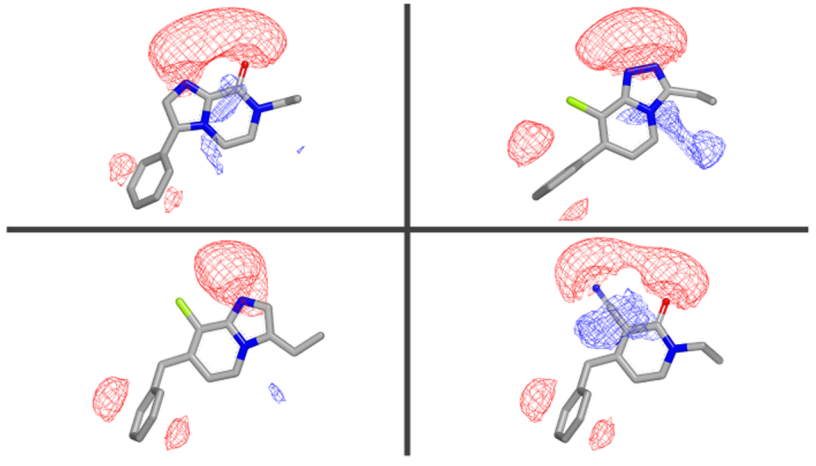

Figure 3. Comparison of the electrostatic fields for the identified imidazopyrazinone scaffold (top left) compared to previously reported triazolopyridine (top right), imidazopyridine (bottom left), and cyanopyridone (bottom right). The red mesh represents negative electrostatic potential, and the blue one, positive.

azinone hit **3a** by the introduction of a focused set of substituents (R) selected from our triazolopyridine series exploration. In a second step, further exploration of the scaffold was conducted as shown in Figure 2.

RESULTS AND DISCUSSION

A scaffold hopping exercise was conducted using computational techniques based on 3D shapes and electrostatic similarity. These methods are suitable for scaffold hopping because they assess properties important for biological recognition and not just underlying atom connectivity. We have previously developed optimal implementations of these approaches[19] and applied them to identify mGlu2 PAM scaffolds.[14,18] Here, our approach was similar and aimed at replacing the central scaffold, the triazolopyridine in **2a**, with alternative heterocyclic ring systems. We have databases of prefragmented compounds from internal and commercial sources and use these to search and retrieve alternative 3D-similar heterocycles. In our approach, the open valences of the query scaffold, the triazolopyridine, and database fragments are

https://doi.org/10.1021/acsomega.1c03739
ACS Omega 2021, 6, 22997−23006

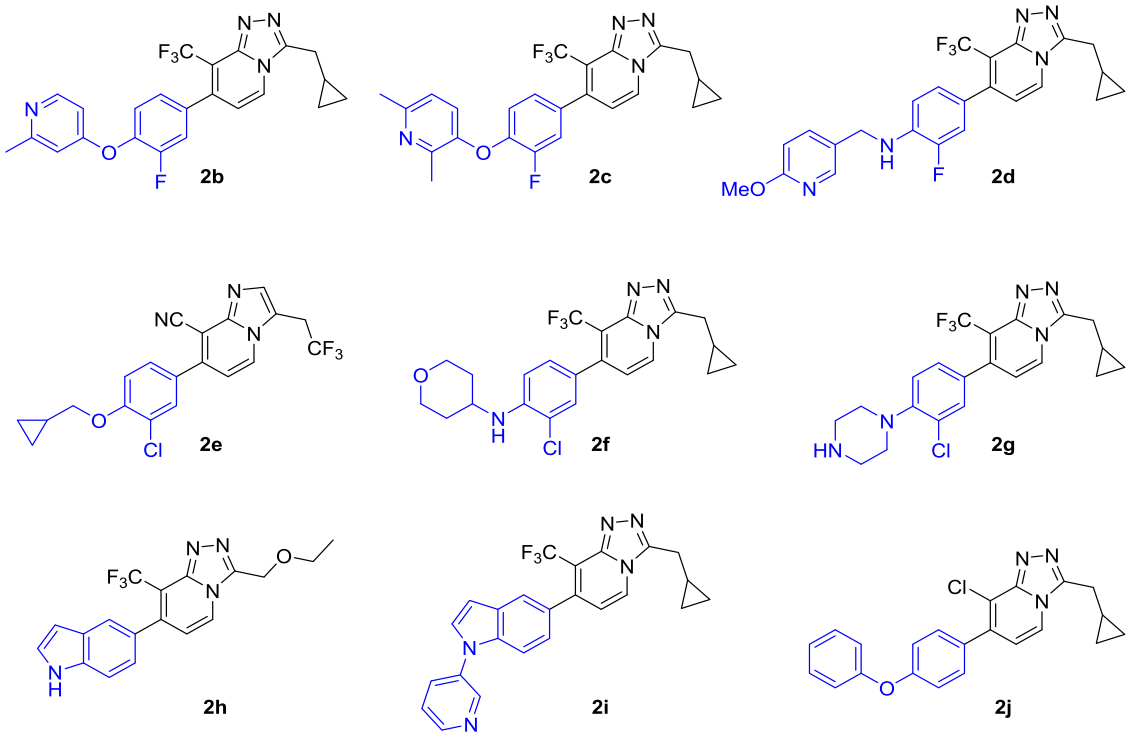

Figure 4. mGlu2 PAM imidazopyridine and triazolopyridines containing a representative set of fragments highlighted in blue, selected to guide exploration on the imidazopiperazinone hit **3a**.

all capped with simple substituents capturing the chemistry of the final molecules; in this case, ethyl and phenyl or benzyl groups represent the right-hand-side and left-hand-side substituents, respectively (Figure 3). The ROCS[20] and EON software from Openeye Scientific[21−25] were used, which assess shape and electrostatic parameters, respectively.

Among the best computational hits was the imidazopyrazinone core that showed remarkably good and visibly clear electrostatic similarity with our previous mGlu2 PAM scaffolds (Figure 3). The ROCS + EON combo scoring function, which is the summation of the Tanimoto similarity scores for shape and electrostatics, ranges from 0 to 2. The shape and electrostatics indicated high similarity of alignment between the two was high, 1.6 between the imidazopyrazinone and the triazolopyridine for example. Furthermore, the new scaffold reproduced important pharmacophoric features.[14] For instance, the scaffold hydrogen bond acceptor feature was present and in an identical position, the adjacent cyano or chloro substituent in previous scaffolds was mimicked by the fused imidazo ring; finally, the substituent vectors on either side of the scaffold were also maintained. Together, this suggested the imidazopyrazinone as a promising starting point for follow-up chemistry.

Given the excellent similarity with previous scaffolds, we hypothesized that the potential SAR around the new imidazopyrazinone core could be broadly consistent with that observed for the imidazopyridine and triazolopyridine cores. To start the exploration of hit **3a**, a set of preferred substituents represented in mGlu2 PAM triazolopyridines **2b−j** were selected (Figure 4, fragments highlighted in blue).

The synthesized imidazopyrazinones **3a−j** along with their mGlu2 PAM functional activity, human and rat liver microsomal stability (HLM and RLM, respectively), and *c* Log *P* are shown in Table 1.

Comparative matched pair analysis confirmed SAR from the imidazo and triazolopyridine series readily transferred to the new imidazopyrazinone core. In general, compounds **3b−j** showed comparable mGlu2 PAM activity to their matched pairs **2b−j** and improved microsomal stability as a result of their reduced lipophilicity.

Replacement of the 4-phenylpiperidine substituent in **3a** with pyridyloxy or pyridylmethylamino fragments from triazolopyridine **2b−d** led to compounds **3b−d**. They had improved mGlu2 PAM activity compared to **3a** and were in the same potency range as their corresponding matched pairs **2b−d**. Likewise, the metabolic stability profile of **3a−d** appeared to be more balanced across human and rat liver microsomes compared to the triazolopyridines **2a−d**, with moderate improvements in rat liver microsomal stability for compounds **3c** and **3d**. Substitution of the imidazopyrazinone core with the alkyl chloroaryl ether present in the imidazopyridine **2e** was beneficial for mGlu2 PAM activity, with compound **3e** being ∼30-fold more potent than **3a**. Finally, compounds **3f−j** were also comparable mGlu2 PAMS to their corresponding matched pairs from the triazolopyridine series, confirming the value of the scaffold hopping approach used to identify novel chemotypes with mGlu2 PAM activity.

With the identification of the imidazopyrazinone core as viable alternative to the triazolopyridine scaffold, we next looked for alternative 5,6-bicyclic scaffolds aiming to further improve the activity and properties of this novel series. For this purpose, compound **3e** was selected as a prototype since it offered good mGlu2 PAM activity and balanced metabolic stability across human and rat liver microsomes.

As shown in Table 2, replacement of the imidazo ring in **3e** by a fused 1,2,4-triazole (**4a**) led to a ∼5-fold decrease in potency (**4a**, mGlu2 PAM EC_{50} = 157 nM vs **3e**, mGlu2 PAM EC_{50} = 28 nM). Scaffold **4b** containing a fused triazinone ring

https://doi.org/10.1021/acsomega.1c03739
ACS Omega 2021, 6, 22997−23006

Table 1. mGlu2 PAM and Agonistic Activity, Human and Rat Microsomal Stability Data, and cLoP for Imidazopyrazinones 3a−j[a,b,c,d,e]

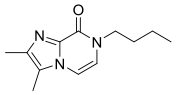

compd	R	mGlu2 PAM[a] EC_{50} (nM) (95% CI)[b]	mGlu2 PAM[a] E_{MAX} (%)[c] ±SD	mGlu2 Ago[a] EC_{50} (nM) (95% CI)[b]	mGlu2 Ago[a] E_{MAX} (%)[c] ±SD	HLM (%)[c]	RLM (%)[c]	cLogP[d]
2a	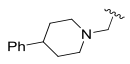	16 (14-19)	263±39	179 (136-235)	43±7	11	84	4.92
3a		490 (448-536)	214	>50,000	42	20	58	3.83
2b[22]	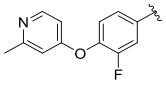	55 (38-80)	269±45	1,862 (1,006-3,448)	77±12	14	29	5.12
3b		24 (16-37)	277	575 (480-689)	90±2	19	37	3.99
2c[17]	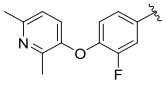	9 (6-14)	362±84	269	101	31	87	5.62
3c		29 (27-31)	248±14	1,820	54	24	56	4.49
2d[17]	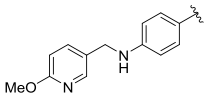	14 (11-17)	262±21	141 (123-162)	64±1	22	93	4.66
3d		73 (60-88)	244±23	571 (363-898)	47±1	59	36	3.71
2e[23]	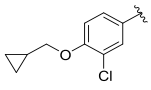	759	209	1,698	30	16	28	5.2
3e		28	322±107	145	49	20	49	4.79
2f[17]	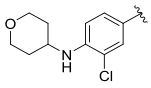	19 (15-23)	353	631	72	18	73	4.43
3f		72 (58-88)	240±6	295	39	23	71	3.46
2g[24]	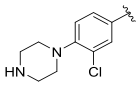	131 (71-242)	308±31	11,954 (8,936-15,990)	68±6	8	23	4.51
3g		174 (131-231)	237±81	989 (449-2,178)	36±4	0	17	3.41
2h[25]		174 (127-238)	269±11	1,738	54	52	97	3.31
3h		166 (97-285)	328	2,512	90	30	97	3.24
2i[17]	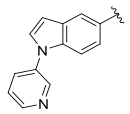	30	424	135	64	22	89	5.7
3i		59 (22-159)	224±41	229	44	35	47	4.57
2j[14]	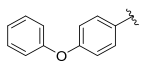	38 (35-42)	225±12	240 (191-301)	50±0	6	10	5.7
3j		15 (11-22)	256±7	151 (121-190)	48±2	2	86	5.04

[a]Effect of compounds on glutamate-induced [^{35}S]GTPγS binding at the mGlu2 receptor in the presence (PAM) and absence (Ago) of an EC_{20} glutamate concentration. [b]Values are the mean of at least two experiments. [c]Values are within a confidence interval of >95%. [d]HLM and RLM data refer to the percentage of compound metabolized after incubation with microsomes for 15 min at a 5 μM concentration. [e]*c* log *P* calculated with Biobyte software.

showed a ∼3-fold decrease in mGlu2 PAM activity (**4b**, mGlu2 PAM EC_{50} = 101 nM vs **3e**, mGlu2 PAM EC_{50} = 28 nM). Shifting one nitrogen in the imidazotriazinone **4b** to isomer **4c** was clearly detrimental for the activity, with **4c** being ∼17-fold less active than **3e** (**4c**, mGlu2 PAM EC_{50} = 484 nM vs **3e**, mGlu2 PAM EC_{50} = 28 nM). The pyrazolotriazinone **4d** showed comparable mGlu2 PAM activity to imidazotriazinone **4b** (**4d**, mGlu2 PAM EC_{50} = 87 nM vs **4b**, mGlu2 PAM EC_{50} = 101 nM). Finally, shifting the position of the nitrogen of the imidazole led to imidazopyrazinone **4e** that was ∼10-fold less potent than **3e**. From this exploration, we concluded that none of the new cores was better tolerated for activity at the mGlu2 receptor than the imidazopyrazinone scaffold in **3e**. Interestingly, the nitrogen count in the 5,6-bicyclic scaffold has a pronounced effect in metabolic stability in human liver microsomes. Thus, compounds **4a−d** containing four nitrogen atoms were more stable than **3e** and **4e** with only three nitrogen atoms. This effect could also be observed in rat liver microsomes, although less pronounced. This observation illustrates the sound medicinal chemistry principle that reducing overall lipophilicity is beneficial for increasing metabolic stability. Moreover, the compounds were evaluated in the absence of glutamate to assess their intrinsic activity. As shown in both Tables 1 and 2, a significant reduction in potency (>1 log unit) was noted and following similar trends observed with their corresponding matched pairs.

https://doi.org/10.1021/acsomega.1c03739
ACS Omega 2021, 6, 22997−23006

Table 2. mGlu2 PAM and Agonistic Activity, Human and Rat Microsomal Stability Data, and cLoP for Core Variations 4a−e[a,b,c,d,e]

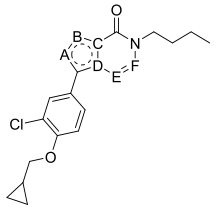

Compd	R	mGlu2 PAM[a] EC_{50} (nM) (95% CI)[b]	mGlu2 PAM[a] E_{MAX} (%)[c] ±SD	mGlu2 Ago[a] EC_{50} (nM) (95% CI)[b]	mGlu2 Ago[a] E_{MAX} (%)[c] ±SD	HLM (%)[d]	RLM (%)[d]	cLogP[e]
3e	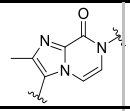	28	322±107	145	49	20	49	4.79
4a	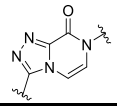	157 (134-183)	272	42,658	53	2	45	3.89
4b	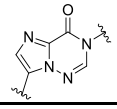	101 (53-195)	211	n.m.	15	1	25	4.15
4c	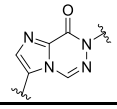	484 (201-1167)	160	>50,119	8	4	21	3.83
4d	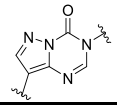	87 (70-109)	226±3	214	35	0	60	3.91
4e	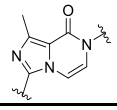	327 (233-459)	151±8	>50,119	12	31	74	5.09

[a]Effect of compounds on glutamate-induced [^{35}S]GTPγS binding at the mGlu2 receptor in the presence (PAM) and absence (Ago) of an EC_{20} glutamate concentration. [b]Values are the mean of at least two experiments. [c]Values are within a confidence interval of >95%. [d]HLM and RLM data refer to the percentage of compound metabolized after incubation with microsomes for 15 min at a 5 μM concentration. [e]*c* log *P* calculated with Biobyte software.

Table 3. In Vitro Functional Effects of 3e on mGlu Receptors

receptor[aP]	PAM EC_{50} (μM)/E_{max} (%)	agonism EC_{50} (μM)/E_{max} (%)	antagonism IC_{50} (μM)/E_{max} (%)
mGlu1 (Ca^{2+})	n.d.[b]	>30/4	>30/18
mGlu2 (Ca^{2+})	0.09/149	0.42/114	n.d.[b]
mGlu2 (GTPγS)	0.028/322	n.d.[b]	n.d.[b]
mGlu3 (Ca^{2+})	14.3/63	>30/2	>30/15
mGlu4 (Ca^{2+})	n.d.[b]	>25/5	17/100
mGlu5 (Ca^{2+})	>30/0	>30/0	>30/7
mGlu6 (GTPγS)	n.d.[b]	>30/1	26.52/53
mGlu7 (Ca^{2+})	>25/5	>25/1	8.32/27
mGlu8 (Ca^{2+})	>25/nd[2]	>25/−4	>25/16

[aP]harmacological read-out used to detect each activity is indicated in brackets. [b]Not determined.

According to the allosteric strategy, all compounds displayed a high level of selectivity toward other mGlu receptor subtypes. Thus, all compounds did not activate or inactivate any of the human mGlu receptor subtypes or the rat mGlu6 receptor at least up to 10 μM, indicating that they selectively modulate the mGlu2 function as illustrated with compound **3e** in Table 3.

Given the good mGlu2 PAM activity and reasonable metabolic stability observed with the original imidazopyrazinone core, in vivo brain penetration studies in rats were performed on compounds **3b−e**, **3h**, and **3j**. Plasma and brain concentrations were measured at 1, 2, and 4 h after dosing at 10 mg/kg. The results obtained are shown in Table 4 along with data for triazolopyridines **2c** and **2d** for comparison.

In general, high plasma exposures after 1 h postdose were observed for all compounds with the exception of **3h** and **3j**. The plasma levels measured were comparable, if not better, to

https://doi.org/10.1021/acsomega.1c03739
ACS Omega 2021, 6, 22997−23006

Table 4. Brain and Plasma Kinetics in Rat after a Single Dose[a]

	plasma level (ng/mL)			brain level (ng/g)			
copd	1 h	2 h	4 h	1 h	2 h	4 h	B/P[c]
2c	564	442	59	464	370	61	0.8
2d	2008	1350	643	730	478	307	0.4
3b[b]	2090	1237	720	405	343	244	0.3
3c	1825	n.d.	n.d.	446	n.d.	n.d.	0.2[f]
3d	1919[e]	n.d.	n.d.	502[e]	n.d.	n.d.	0.3[e]
3e	1417	1389	526	2537	2859	835	2.0
3h[b]	19	44	42	BQL	10	12	0.2
3j[b]	263	192	14	104	92	BQL[d]	0.5

[a]Study in male Sprague Dawley rat (n = 1) dosed at 10 mg/kg s.c. in solution (20% HP-β-CD at pH 3). [b]10 mg/kg dose p.o. [c]B/P is the ratio between brain and plasma concentration after 2 h. [d]Below quantification limits. [e]Value after 1.5 h. [f]Value after 1 h.

those observed for the triazolopyridine series, as seen by comparing the matched pairs **2c**/**3c** and **2d**/**3d**. The measured plasma concentrations indicate acceptable absorption properties for the new imidazopyrazinone scaffold. Matched pair analysis also shows that compound brain levels measured after 1 h administration were also comparable. Compound **3e** exhibited the most optimal pharmacokinetic profile of all analogues evaluated, displaying the highest plasma and brain exposures with a favorable B/P ratio. Although compounds distributed preferentially to plasma over brain, the good B/P ratio observed with compound **3e** suggests that brain-penetrant compounds can be found within the imidazopyrazinone series by modulating the substitution pattern on the bicyclic core.

CONCLUSIONS

In summary, the discovery and scaffold exploration of a novel series of imidazopyrazinone mGlu2 receptor PAM is reported. The hit scaffold originated by computational searching of fragment databases and comparison with our previously explored triazolopyridine, imidazopyridine, and cyanopyridone scaffolds. We again show the utility and importance of in silico scaffold hopping using 3D shapes and electrostatic methods. Our robust understanding of the SAR and important pharmacophoric features helped readily identify the preferred scaffold. The exploration led to compound **3e**, which showed good potency and selectivity toward other mGlu receptor subtypes as well as a reasonable metabolic stability and good brain exposure. All of these attributes make **3e** a suitable compound to progress to in vivo studies.

EXPERIMENTAL SECTION

The synthetic procedure for the preparation of imidazo[1,2-*a*]pyrazin-8-ones (**3a**−**j**) is outlined in Scheme 1 and subsequent warhead variations **4a**−**e** are outlined in scheme 2−6, respectively.

Compounds **3a**−**j** (Scheme 1) were synthesized from common intermediate **5**.[26] Thus, the treatment of **5** with HCl resulted in **6**, which was then treated with bromobutane to yield the *N*-alkylated product **7**. Reaction of **7** with vinylboronic acid pinacol ester under Suzuki coupling conditions led to vinylimidazopyrazinone **8**. Oxidation of the vinyl group in **8** with $NaIO_4$ and OsO_4 gave the corresponding aldehyde **9**. Subsequent reaction with 4-phenylpiperidine under reductive amination conditions provided final compound **3a**. Compounds **3b**−**j** were prepared in one step from intermediate compound **7** by Suzuki−Miyaura coupling with the corresponding arylboronic pinacol ester or acid (**10b**−**j**).[12]

Synthesis of compounds **4a**−**e** required the design and execution of specific synthetic routes as shown in scheme 2−6. The preparation of target compound **4a** (Scheme 2) started from commercially available 2,3-dichloropyrazine, which was first monoprotected with cyclohexanol to give intermediate **11** and then selectively hydrolyzed to pyrazinone **12**. Subsequent *N*-alkylation with 1-bromobutane afforded **13**. Cleavage of the protecting group and chlorination were achieved in one step

Scheme 1. General Synthesis of Imidazo[1,2-*a*]pyrazin-8-ones 3a−j[a]

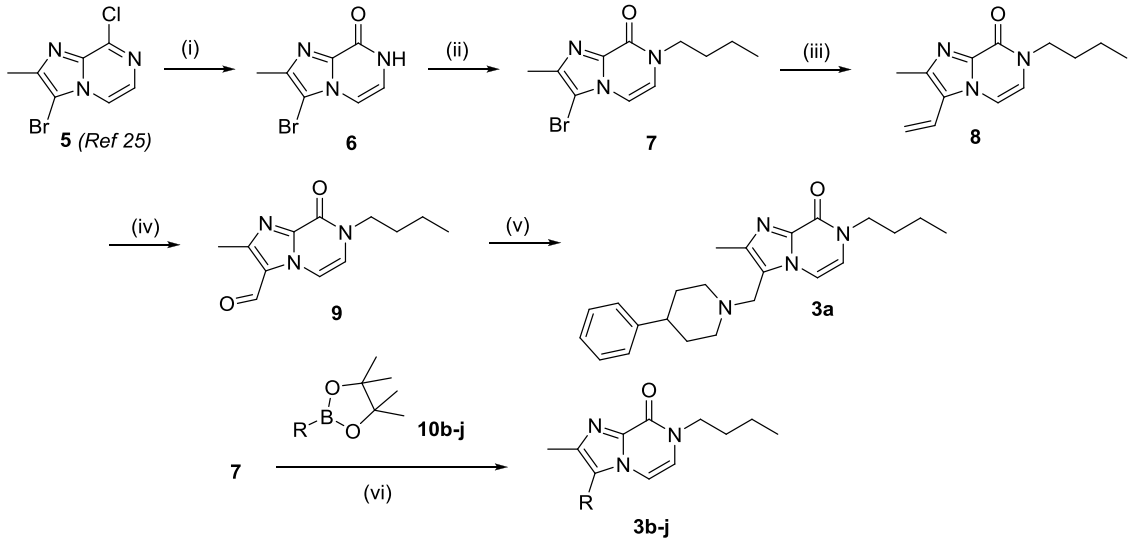

[a]Reagents and conditions: (i) HCl (37%), 90 °C for 4 h. Y: 81%. (ii) 1-Bromobutane, Cs_2CO_3, 1,4-dioxane, 90 °C, 48 h. Y: 98%. (iii) Vinylboronic acid pinacol ester, $Pd(PPh_3)_4$, $NaHCO_3$, 1,4-dioxane, MW, 150 °C, 10 min. Y: 59%; (iv) $NaIO_4$, OsO_4,1,4-dioxane/water, rt, 2 h. Y: 65%. (v) 4-Phenylpiperidine, $NaBH(OAc)_3$, DCE, rt,16 h. Y: 28%. (vi) $Pd(PPh_3)_4$, $NaHCO_3$ (aq.), 1,4-dioxane, MW, 150 °C, 40 min. Y: 30−88%. See the Supporting Information for detailed protocols.

https://doi.org/10.1021/acsomega.1c03739
ACS Omega 2021, 6, 22997−23006

Scheme 2. Synthesis of 7-Butyl-3-[3-chloro-4-(cyclopropylmethoxy)phenyl]-[1,2,4]triazolo[4,3-*a*]pyrazin-8-one[a]

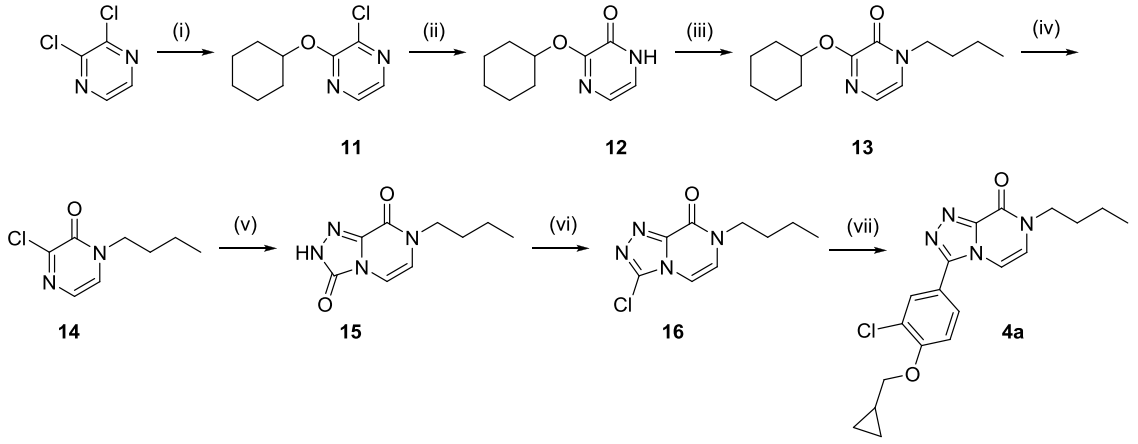

[a]Reagents and conditions: (i) NaH, cyclohexanol, 1,2-dimethoxyethane, reflux, 30 min. Y: 90%. (ii) NaOH, DMSO, 90 °C, 2 h. Y: 45%. (iii) 1-Bromobutane, K_2CO_3, MeCN, MW, 140 °C, 40 min. Y: 77%. (iv) $POCl_3$, DCM, MW, 150 °C, 20 min. Y: 60%. (v) Ethyl carbazate, propionitrile, MW, 190 °C, 30 min. Y: 87%. (vi) $POCl_3$, 110 °C, 22 h, Y: 35%. (vii) $Pd(PPh_3)_4$, 2-[3-chloro-4-(cyclopropylmethoxy)-phenyl]-4,4,5,5-tetramethyl-1,3,2-dioxaborolane, $NaHCO_3$, dioxane, MW, 150 °C, 10 min. Y: 83%. See the Supporting Information for detailed protocols.

Scheme 3. Synthesis of 3-Butyl-7-[3-chloro-4-(cyclopropylmethoxy)phenyl]imidazo[2,1-*f*][1,2,4]triazin-4-one[a]

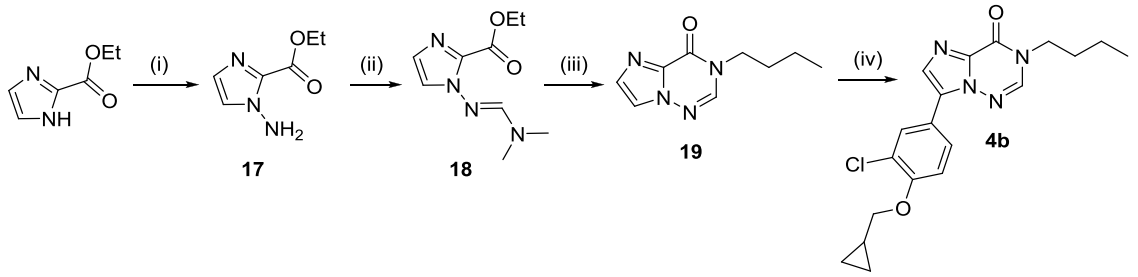

[a]Reagents and conditions: (i) *o*-diphenylphosphinylhydroxylamine, Cs_2CO_3, rt, 20 min. Y: 99%. (ii) *N*,*N*-dimethylformamide dimethyl acetal, propionitrile, MW, 120 °C, 15 min. Y: 97%. (iii) 1-Butylamine, propionitrile, MW, 180 °C, 50 min. Y: 38%; (iv) $Pd(OAc)_2$, 4-bromo-2-chloro-1-(cyclopropylmethoxy)-benzene, PPh_3, AcOK, DMA, 120 °C, 30 h. Y: 35%. See the Supporting Information for detailed protocols.

Scheme 4. Synthesis of 7-Butyl-3-[3-chloro-4-(cyclopropylmethoxy)phenyl]imidazo[1,2-*d*][1,2,4]triazin-8-one[a]

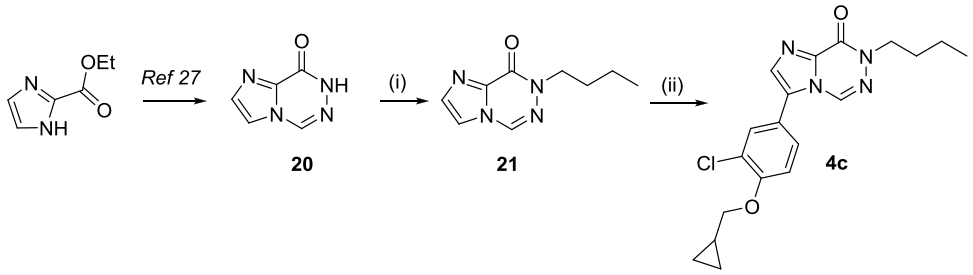

[a]Reagents and conditions: (i) NaH, DME, DMF, LiBr, 1-iodobutane, MW, 150 °C, 5 min. Y: 35%. (ii) $Pd(OAc)_2$, 4-bromo-2-chloro-1-(cyclopropylmethoxy)-benzene, PPh_3, AcOK, DMA, 120 °C, 30 h. Y: 55%. See the Supporting Information for detailed protocols.

using phosphorus oxychloride leading to compound **14**. Cyclization of **14** with ethyl carbazate gave bicyclic **15** in good yield. The treatment of **15** with phosphorus oxychloride followed by Suzuki coupling resulted in the final compound **4a**. Imidazotriazinone **4b** was synthesized via amination of 1*H*-imidazole-2-carboxylic acid and ethyl ester (Scheme 3). The amination product **17** was condensed with *N*,*N*-dimethylformamide dimethyl acetal to afford formimidamide **18**, which by thermal cyclization led to imidazotriazinone intermediate **19**. Subsequent coupling with the corresponding bromoarene afforded the C−H coupling product **4b** under Heck reaction conditions. Synthesis of **4c** (Scheme 4) was carried out via *N*-alkylation of intermediate **20**[27] and subsequent reaction of **21** via C−H coupling with a corresponding bromoaryl reactant. Compound **4d** (Scheme 5) was prepared from commercially available 3-amino-5-methylpyrazole, which was first treated with butyl isocyanate to afford **22** and then cyclized with ethylorthoformate to produce **23**. Subsequent regioselective bromination of **23** led to **24** that was reacted with the corresponding boronic acid pinacol ester under Suzuki conditions to furnish final compound **4d**. Finally, compound **4e** (Scheme 6) was prepared by benzoylation of **25**[28] to intermediate **26**, followed by $POCl_3$-mediated cyclization to afford the bicyclic intermediate **27**, which after hydrolysis

https://doi.org/10.1021/acsomega.1c03739
ACS Omega 2021, 6, 22997−23006

Scheme 5. Synthesis of 3-Butyl-8-[3-chloro-4-(cyclopropylmethoxy)phenyl]-7-methyl-pyrazolo[1,5-*a*][1,3,5]triazin-4-one[a]

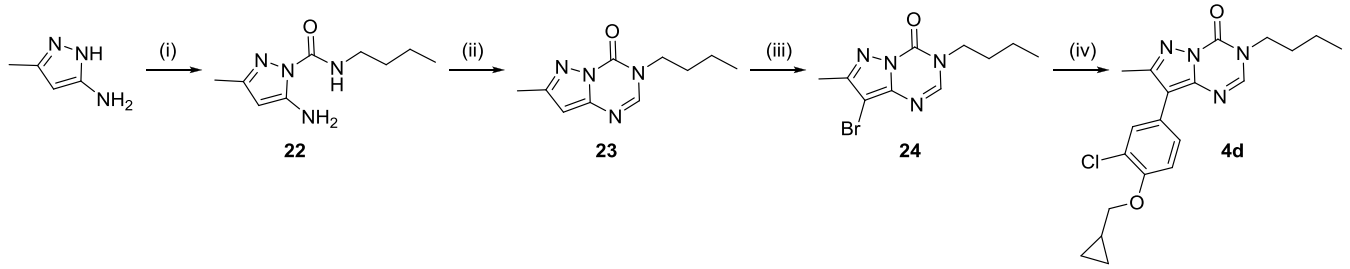

[a]Reagents and conditions: (i) DIPEA, butyl isocyanate, acetone 50 °C. 2 h, Y: 89%. (ii) Triethyl orthoformate, DMF, MW, 160 °C, 40 min. Y: 38%. (iii) NBS, DMF, 50 °C, 1 h. Y: 63%. (iv) $Pd(PPh_3)_4$, 3-chloro-4-(cyclopropylmethoxy)-phenylboronic acid pinacol ester, $NaHCO_3$, dioxane, MW, 150 °C, 10 min. Y: 73%. See the Supporting Information for detailed protocols.

Scheme 6. Synthesis of 7-Butyl-3-[3-chloro-4-(cyclopropylmethoxy)phenyl]-1-methyl-imidazo[1,5-*a*]pyrazin-8-one[a]

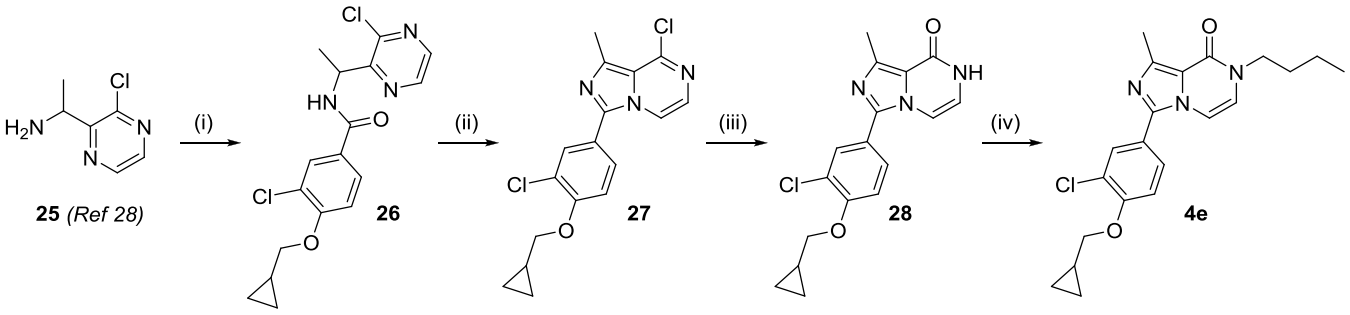

[a]Reagents and conditions: (i) HATU, 3-chloro-4-(cyclopropylmethoxy)-benzoic acid, DIPEA, DMF, rt, 24 h, Y: 79%. (ii) $POCl_3$, toluene, reflux, 4 h. Y: 52%; (iii) NaOH, DMSO, 120 °C, 4 h, Y: 83%. (iv) 1-Bromobutane, K_2CO_3, MeCN, MW, 170 °C, 40 min. Y: 62%. See the Supporting Information for detailed protocols.

under basic conditions led to the desired intermediate **28**. Alkylation of **28** with 1-bromobutane resulted in the desired final compound **4e** with moderate yield.

■ ASSOCIATED CONTENT

Supporting Information

The Supporting Information is available free of charge at https://pubs.acs.org/doi/10.1021/acsomega.1c03739.

Assay protocols, experimental procedures, and analytical data for compounds **3a−j**, **4a−e**, and **5−28** (PDF)

■ AUTHOR INFORMATION

Corresponding Authors

Ana I. de Lucas − *Discovery Chemistry, Discovery Sciences, Janssen Research & Development, Division of Janssen-Cilag S.A., Toledo 45007, Spain*; Phone: +34 925 245768; Email: adelucas@its.jnj.com

José M. Cid − *Discovery Chemistry, Discovery Sciences, Janssen Research & Development, Division of Janssen-Cilag S.A., Toledo 45007, Spain*; orcid.org/0000-0002-4774-8361; Phone: +34 925 245767; Email: jcid@its.jnj.com

Authors

Juan A. Vega − *Discovery Chemistry, Discovery Sciences, Janssen Research & Development, Division of Janssen-Cilag S.A., Toledo 45007, Spain*

Aránzazu García Molina − *Discovery Chemistry, Discovery Sciences, Janssen Research & Development, Division of Janssen-Cilag S.A., Toledo 45007, Spain*

María Lourdes Linares − *Discovery Chemistry, Discovery Sciences, Janssen Research & Development, Division of Janssen-Cilag S.A., Toledo 45007, Spain*

Gary Tresadern − *Computational Chemistry, Discovery Sciences, Janssen Research & Development, Division of Janssen Pharmaceutica N.V., B-2340 Beerse, Belgium*; orcid.org/0000-0002-4801-1644

Hilde Lavreysen − *Clinical Research and Development, Janssen Pharmaceutica N.V., B-2340 Beerse, Belgium*

Daniel Oehlrich − *Discovery Chemistry, Discovery Sciences, Janssen Research & Development, Division of Janssen Pharmaceutica N.V., B-2340 Beerse, Belgium*; orcid.org/0000-0002-3392-1952

Andrés A. Trabanco − *Discovery Chemistry, Discovery Sciences, Janssen Research & Development, Division of Janssen-Cilag S.A., Toledo 45007, Spain*; orcid.org/0000-0002-4225-758X

Complete contact information is available at: https://pubs.acs.org/10.1021/acsomega.1c03739

Author Contributions

The manuscript was written through contributions of all authors. All authors have given approval to the final version of the manuscript.

Notes

The authors declare no competing financial interest.

■ ACKNOWLEDGMENTS

The authors thank members of the purification and analysis team from Toledo and the biology and ADMET team from Janssen R&D.

ABBREVIATIONS

mGlu2, metabotropic glutamate 2; PAM, positive allosteric modulator; GPCR, G-protein-coupled receptor; CNS, central nervous system; HTS, high-throughput screening; SAR, structure−activity relationship; RLM, rat liver microsomes; HLM, human liver microsomes

REFERENCES

(1) Kew, J. N. C.; Kemp, J. A. Ionotropic and metabotropic glutamate receptor structure and pharmacology. *Psychopharmacology* **2005**, *179*, 4−29.

(2) Pin, J. P.; Galvez, T.; Prezeau, L. Evolution, structure, and activation mechanism of family 3/C G-protein-coupled receptors. *Pharmacol. Ther.* **2003**, *98*, 325−354.

(3) Szabo, G.; Keseru, G. M. Positive allosteric modulators for mGlu2 receptors: a medicinal chemistry perspective. *Curr. Top. Med. Chem.* **2014**, *14*, 1771−1788.

(4) Trabanco, A. A.; Cid, J. mGluR2 positive allosteric modulators: a patent review (2009 - present). *Expert Opin. Ther. Pat.* **2013**, *23*, 629−647.

(5) Trabanco, A. A.; Cid, J. M.; Lavreysen, H.; Macdonald, G. J.; Tresadern, G. Progress in the development of positive allosteric modulators of the metabotropic glutamate receptor 2. *Curr. Med. Chem.* **2011**, *18*, 47−68.

(6) Di Prisco, S.; Elisa, M.; Tommaso, O.; Cervetto, C.; Grilli, M.; Usai, C.; Marchi, M.; Pittaluga, A.; et al. Presynaptic, release-regulating mGlu2-preferring and mGlu3-preferring autoreceptors in CNS: pharmacological profiles and functional roles in demyelinating disease. *Br. J. Pharmacol.* **2016**, *173*, 1465−1477.

(7) Brauner-Osborne, H.; Wellendorph, P.; Jensen, A. A. Structure, pharmacology and therapeutic prospects of family C G-protein coupled receptors. *Curr. Drug Targets* **2007**, *8*, 169−184.

(8) Metcalf, C. S.; Klein, B. D.; Smith, M. D.; Pruess, T.; Ceusters, M.; Lavreysen, H.; Pype, S.; Van Osselaer, N.; Twyman, R.; White, H. S. Efficacy of mGlu2-positive allosteric modulators alone and in combination with levetiracetam in the mouse 6 Hz model of psychomotor seizures. *Epilepsia* **2017**, *58*, 484−493.

(9) Metcalf, C. S.; Klein, B. D.; Smith, M. D.; Ceusters, M.; Lavreysen, H.; Pype, S.; Van Osselaer, N.; Twyman, R.; White, H. S. Potent and selective pharmacodynamic synergy between the metabotropic glutamate receptor subtype 2−positive allosteric modulator JNJ-46356479 and levetiracetam in the mouse 6-Hz (44-mA) model. *Epilepsia* **2018**, *59*, 724−735.

(10) Lavreysen, H.; Langlois, X.; Ver Donck, L.; Cid Nuñez, J. M.; Pype, S.; Lütjens, R.; Megens, A. Preclinical evaluation of the antipsychotic potential of the mGlu2-positive allosteric modulator JNJ-40411813. *Pharmacol. Res. Perspect.* **2015**, 3, No. e00097.

(11) Salih, H.; Anghelescu, I.; Kezic, I.; Sinha, V.; Hoeben, E.; Van Neuten, L.; De Smedt, H.; De Boer, P. Pharmacokinetic and pharmacodynamic characterization of JNJ-40411813, a positive allosteric modulator of mGluR2, in two randomised, double-blind phase-I studies. *J. Psychopharmacol.* **2015**, *29*, 414−425.

(12) Hilde, L.; Abdellah, A.; Wilhelmus, D.; Xavier, L.; Claire, M.; Stefan, P.; Robert, L.; Emmanuel, L.; Trabanco, A. A.; Jose María, C. N. Pharmacological and pharmacokinetic properties of JNJ-40411813, a positive allosteric modulator of the mGlu2 receptor. *Pharmacol. Res. Perspect.* **2014**, *3*, 1−15.

(13) Cid, J. M.; Tresadern, G.; Duvey, G.; Lutjens, R.; Finn, T.; Rocher, J.-P.; Imogai, H.; Poli, S.; Vega, J.; de Lucas, A. I.; Matesanz, E.; Linares, M. L.; Andrés, J. I.; Alcazar, J.; Macdonald, G. J.; Oehlrich, D.; Lavreysen, H.; Ahnaou, A.; Drinkenburg, W.; Mackie, C.; Pype, S.; Gallacher, D.; Trabanco, A. A. Discovery of 1-butyl-3-chloro-4-(4-phenyl-1-piperidinyl)-(1H)-pyridone (JNJ-40411813): a novel positive allosteric modulator of the metabotropic glutamate 2 receptor. *J. Med. Chem.* **2014**, *57*, 6495−6512.

(14) Tresadern, G.; Cid, J. M.; Macdonald, G. J.; Vega, J. A.; de Lucas, A. I.; García, A.; Matesanz, E.; Linares, M. L.; Oehlrich, D.; Lavreysen, H.; Biesmans, I.; Trabanco, A. A. Scaffold hopping from pyridones to imidazo[1,2-a]pyridines. New positive allosteric modulators of metabotropic glutamate 2 receptor. *Bioorg. Med. Chem. Lett.* **2010**, *20*, 175−179.

(15) Trabanco, A. A.; Tresadern, G.; Macdonald, G. J.; Vega, J. A.; de Lucas, A. I.; Matesanz, E.; García, A.; Linares, M. L.; Alonso de Diego, S:A.; Alonso, J. M.; Oehlrich, D.; Ahnaou, A.; Drinkenburg, W.; Mackie, C.; Andrés, J. I.; Lavreysen, H.; Cid, J. M. Imidazo[1,2-a]pyridines: orally active positive allosteric modulators of the metabotropic glutamate 2 receptor. *J. Med. Chem.* **2012**, *55*, 2688−2701.

(16) Cid, J. M.; Tresadern, G.; Vega, J. A.; De Lucas, A. I.; Matesanz, E.; Iturrino, L.; Linares, M. L.; García, A.; Andrés, J. I.; Macdonald, G. J.; Oehlrich, D.; Lavreysen, H.; Megens, A.; Ahnaou, A.; Drinkenburg, W.; Mackie, C.; Pype, S.; Gallacher, D.; Trabanco, A. A. Discovery of 3-cyclopropylmethyl-7-(4-phenyl-piperidin-1-yl)-8-trifluoromethyl-[1,2,4]triazolo[4,3-a] pyridine (JNJ-42153605): A positive allosteric modulator of the metabotropic glutamate 2 receptor. *J. Med. Chem.* **2012**, *55*, 8770−8789.

(17) Cid, J. M.; Tresadern, G.; Vega, J. A.; de Lucas, A. I.; del Cerro, A.; Matesanz, E.; Linares, M. L.; García, A.; Iturrino, L.; Pérez-Benito, L.; Macdonald, G. J.; Oehlrich, D.; Lavreysen, H.; Peeters, L.; Ceusters, M.; Ahnaou, A.; Drinkenburg, W.; Mackie, C.; Somers, M.; Trabanco, A. A. Discovery of 8-trifluoromethyl-3-cyclopropylmethyl-7-[(4-(2,4-difluorophenyl)-1-piperazinyl)methyl]-1,2,4-triazolo[4,3-a]pyridine (JNJ-46356479), a selective and orally bioavailable mGlu2 receptor positive allosteric modulator (PAM). *J. Med. Chem.* **2016**, *59*, 8495−8507.

(18) de Lucas, A. I.; Vega, J. A.; Matesanz, E.; Linares, M. L.; Garcia Molina, A.; Tresadern, G.; Lavreysen, H.; Trabanco, A. A.; Cid, J. M. Spiro-oxindole piperidines and 3-(azetidin-3-yl)-1H-benzimidazol-2-ones as mGlu2 receptor PAMs. *ACS Med. Chem. Lett.* **2020**, *11*, 303−308.

(19) Tresadern, G.; Bemporad, D.; Howe, T. A comparison of ligand based virtual screening methods and application to corticotropin releasing actor 1 receptor. *J. Mol. Graphics Modell.* **2009**, *27*, 860−870.

(20) Hawkins, P. C. D.; Skillman, A. G.; Nicholls, A. comparison of shape-matching and docking as virtual screening Tools. *J. Med. Chem.* **2007**, *50*, 74−82.

(21) ROCS version 3.2.0.4, EON version 2.2.0.5; OpenEye Scientific Software: Santa Fe, NM, 2013.

(22) Doornbos, M. L. J.; Cid, J. M.; Haubrich, J.; Nunes, A.; van de Sande, J. W.; Vermond, S. C.; Mulder-Krieger, T.; Tra-banco, A. A.; Ahnaou, A.; Drinkenburg, W. H.; Lavreysen, H.; Heitman, L. H.; IJzerman, A. P.; Tresadern, G. Discovery and kinetic profiling of 7-aryl-1,2,4-triazolo[4,3-a]pyridines: positive allosteric modulators of the metabotropic glutamate receptor 2. *J. Med. Chem.* **2017**, *60*, 6704−6720.

(23) Trabanco-Suárez, A. A.; Tresadern, G. J.; Vega-Ramiro, J. A.; Cid-Nuñez, J. M. Preparation of Imidazopyridine Derivatives for Use as Mglur2 Receptor Modulators. Patent WO2009062676 A2, 2009.

(24) Cid-Nuñez, J. M.; De Lucas-Olivares, A. I.; Trabanco-Suárez, A. A.; Macdonald, G. J. 7-Aryl-1,2,4-triazolo[4,3-a]pyridine Derivatives and Their Use as Positive Allosteric Modulators of Mglur2 Receptors. Patent WO2010130423 A1, 2010.

(25) Cid-Nuñez, J. M.; De Lucas-Olivares, A. I.; Trabanco-Suárez, A. A.; Macdonald, G. J. 1,2,4-Triazolo[4,3-a]pyridine Derivatives and Their Use as Positive Allosteric Modulators of Mglur2 Receptors. Patent WO2010130422 A1, 2010.

(26) Bartolomé-Nebreda, J. M.; Delgado, F.; Martin-Martin, M. L.; Martinez-Viturro, C. M.; Pastor, J.; Tong, H. M.; Iturrino, L.; Macdonald, G. J.; Sanderson, W.; Megens, A.; et al. Discovery of a potent, selective, and orally active phosphodiesterase 10A inhibitor for the potential treatment of cchizophrenia. *J. Med. Chem.* **2014**, *57*, 4196−4212.

(27) Goodacre, S. C.; Hallett, D. J.; Carling, R. W.; Castro, J. L.; Reynolds, D. S.; Pike, A.; Wafford, K. A.; Newman, R.; Atack, J. R.; Street, L. J. Imidazo[1,2-a]pyrazin-8-ones, imidazo[1,2-d][1,2,4]-triazin-8-ones and imidazo[2,1-f][1,2,4]triazin-8-ones as $\alpha2/\alpha3$

https://doi.org/10.1021/acsomega.1c03739
ACS Omega 2021, 6, 22997−23006

subtype selective GABAA agonists for the treatment of anxiety. *Bioorg. Med. Chem. Lett.* **2006**, *16*, 1582−1585.
(28) Schaetzer, J. H.; Edmunds, A.; Gagnepain; Julien, D. H.; Hall, R. G.; Jeanguenat; Andre; Kolleth Krieger, A.; Le Chapelain, C.; Palwe, S.; Phadte, M.; Pitterna, T.; Rendler, S.; Scarborough, C. C. Preparation of Pesticidally Active Diazine-Amide Compounds. Patent WO WO2020208036, 2020.

https://doi.org/10.1021/acsomega.1c03739
ACS Omega 2021, 6, 22997−23006